RSC Advances

PAPER

View Article Online
View Journal | View Issue

Cite this: *RSC Adv.*, 2017, **7**, 28489

A highly versatile fluorenone-based macrocycle for the sensitive detection of polycyclic aromatic hydrocarbons and fluoride anions†

Ingrid-Suzy Tamgho,‡ Sauradip Chaudhuri,‡ Molly Verderame, Dana J. DiScenza and Mindy Levine *

Received 12th May 2017
Accepted 23rd May 2017

DOI: 10.1039/c7ra05404a

rsc.li/rsc-advances

Reported herein is the high yielding synthesis of a new fluorenone-based triazolophane and its sensing capabilities for polycyclic aromatic hydrocarbons (PAHs) and fluoride anions. Fluorescence, UV/Vis and ^{1}H NMR spectroscopy results showed the triazolophane has a high sensitivity for selected PAHs and binds the fluoride anion in a 2 : 1 stoichiometry *via* C–H hydrogen bonding with the triazole and fluorenone protons.

Cyclophanes, or macrocycles that contain aromatic rings linked by aliphatic chains, have been studied in the literature for a range of applications.[1] These macrocycles can bind a variety of guests in their interiors, including polycyclic aromatic hydrocarbons (PAHs)[2] as well as anions[3] and cations,[4] through multiple non-covalent interactions. Since the synthesis of the simplest cyclophane, [2.2]paracyclophane, in 1966,[5] the number of known cyclophanes has expanded dramatically.

Recent cyclophanes have replaced one or more of the aromatic rings with heteroaromatic moieties,[6] including triazole rings for the formation of triazolophane macrocycles.[7] Such macrocycles are attractive because of the synthetic accessibility of triazoles[8] as well as their ability to bind both cations (*via* association with the N2 and N3 of the triazole)[9] and anions (*via* hydrogen bonding with the C–H hydrogen bond donor).[10]

Anions are important targets for binding and detection due to their ubiquitous nature and public health relevance.[11] Fluoride, for example, is of interest due to the importance of fluoridated water in promoting dental health;[12] excessive amounts of fluoride, by contrast, can lead to fluorosis.[13] Other key anions include those with negative health effects including phosphate,[14] nitrate,[15] thiocyanate[16] and cyanide.[17] A third class of anions is those that are explosive such as azide.[18]

Polycyclic aromatic hydrocarbons (PAHs) are another class of important detection targets, with negative health and environmental effects,[19] and are formed from the incomplete combustion of petroleum.[20] Their environmental stability means that they bioaccumulate and biomagnify,[21] which is of concern due to their known and suspected teratogenicity,[22] mutagenicity[23] and carcinogenicity.[24]

Work in the Levine group has focused on the detection of toxicants using cyclodextrin-promoted energy transfer[25] and cyclodextrin-promoted fluorescence modulation,[26] as well as on the use of synthetic macrocycles for the enhanced binding and detection of PAHs.[27] One shortcoming is that the previously synthesized macrocycles lacked easily detectable photophysically active components, which in turn meant that an external fluorophore was required to obtain a response signal. Incorporating a UV-active moiety, such as fluorenone, directly into the backbone of the macrocycle would enable the direct use of optical detection methods, and incorporation of a triazole functionality will enable the detection of a broader variety of analytes. Reported herein is the high yielding synthesis of precisely such a macrocycle, compound **1**, containing a photophysically active fluorenone unit and two triazole moieties, and its versatility in binding and detecting both PAHs and anions with extremely high sensitivities.

Macrocycle **1** was synthesized from compounds **2** and **3** *via* a copper catalyzed azide–alkyne cycloaddition (Fig. 1). This reaction proceeded under high dilution conditions[28] in toluene to obtain a 71% isolated yield. The low solubility of the macrocycle in toluene caused it to crash out of the reaction mixture, and was crucial in enabling high yields. The formation of the

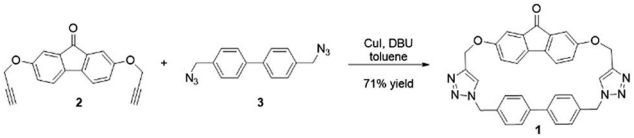

Fig. 1 Synthesis of macrocycle **1** *via* the reaction of precursors **2** and **3**.

Department of Chemistry, University of Rhode Island, 140 Flagg Road, Kingston, RI 02881, USA. E-mail: mlevine@chm.uri.edu; Fax: +1-401-874-5072; Tel: +1-401-874-4243

† Electronic supplementary information (ESI) available: Synthetic procedures, spectral characterization of compounds **1–3**, experimental methods for all photophysical experiments, copies of all spectra, LOD procedures and data. See DOI: 10.1039/c7ra05404a

‡ These authors contributed equally to this work.

macrocycle was confirmed by NMR spectroscopy and mass spectrometry (see ESI†).

Photophysical characterization of the macrocycle showed a UV-visible absorption spectrum with maxima at 264, 310, and 460 nm, corresponding to the π–π* transition of the biphenyl,[29] the electronic transition of the fluorenone,[30] and the symmetry forbidden n–π* transition of the carbonyl moiety,[31] respectively.

DFT calculations of macrocycle **1** showed a well-defined cavity with dimensions of 10.6 Å × 5.043 Å, with the most stable conformation of the macrocycle having the triazole protons facing opposite sides (*i.e.* one pointed out of the page and one pointed into the page) (Fig. 2A). Electron density mapping highlighted the strongly electron deficient nature of the macrocycle, making it well-suited for the binding of electron rich aromatic guests (Fig. 2B).

The binding of polycyclic aromatic hydrocarbons **4–7** (Fig. 3) in macrocycle **1** was monitored by UV-visible and fluorescence spectroscopy. In the UV-visible spectra, the absorbance spectrum of the 1 : 1 mixture of each analyte and macrocycle **1** was equivalent to the sum of the absorbance spectra of the individual species, indicating no significant complexation-induced absorption changes.

In contrast to the limited changes in the absorbance spectra, the fluorescence emission of each of the analytes decreased with the addition of the macrocycle (Table 1), with the decrease in fluorescence quantified according to eqn (1):

$$\text{Fluorescence change} = (\text{Fl}_\text{m} - \text{Fl}_\text{a})/\text{Fl}_\text{a} \times 100 \quad (1)$$

where Fl_a is the integrated fluorescence emission of the analyte and Fl_m is the integrated fluorescence emission of the analyte in the presence of compound **1**.

Of note, these decreases were not accompanied by significant shifts in the emission maxima, in contrast to a report of an analogous system in which such a red shift is observed.[32] In that case, the red-shift is probably a result of excited state energy transfer between the anthracene host and guanine guest.

A direct comparison of the fluorescence changes observed in the presence of macrocycle **1** with those observed in the presence of both photophysically active components – 2,7-dihydroxy-9-fluorenone and 4,4′-dimethylbiphenyl (compounds **8** and **9**, Fig. 4) indicate that the macrocycle induced fluorescence changes were markedly different from those induced by the components in a mixture (Table 1, Fig. 5), thereby supporting the proposed analyte-macrocycle complexation. For

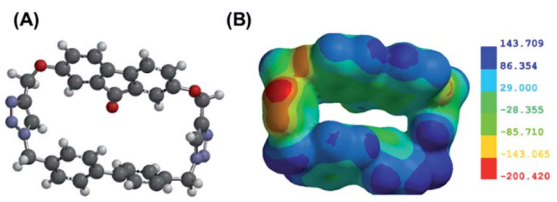

Fig. 2 (A) Energy minimized structure of compound **1**; (B) electron density mapping of compound **1**, with the blue regions corresponding to the electron-deficient segments and the red regions corresponding to the electron-rich segments.

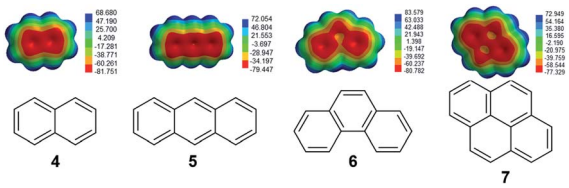

Fig. 3 Structures of polycyclic aromatic hydrocarbons **4–7** with electron density mapping of each compound highlighting their electron rich aromatic natures.

Table 1 Decreases in fluorescence of analytes **4–7** in the presence of compound **1**[a]

Analyte	With macrocycle **1**	With compounds **8** and **9**
4	[b]	[b]
5	−8.5 ± 0.4	−84.6 ± 0.3
6	−11.9 ± 0.3	63.5 ± 1.8
7	−6.0 ± 0.4	19.6 ± 6.2

[a] Fluorescence decreases were calculated according to eqn (1). All results represent an average of 3 trials. [b] Inner filter effects observed.

analyte **5**, the presence of both **8** and **9** led to noticeable fluorescence quenching as a result of intermolecular co-facial aromatic interactions between the anthracene and fluorenone[33] and the anthracene and biphenyl,[34] in accordance with literature precedents of analogous quenching phenomena. Once these moieties are geometrically constrained in a macrocycle (Fig. 2), they are no longer completely planar and are not as available for co-facial quenching interactions. Binding of analyte **5** in macrocycle **1**, as a result, leads to a much more limited decrease in the observed fluorescence emission.

In the case of analytes **6** and **7**, slight fluorescence decreases were observed in the presence of macrocycle **1**, while significant fluorescence enhancements were observed in the presence of both **8** and **9**. These results indicate different interactions of the macrocycle with analytes **6** and **7** compared to its interactions with **4** and **5**. As a result of the larger dimensions of **6** and **7**, there is likely weaker binding in the cavity; as a result, limited fluorescence quenching occurred.

In the case of naphthalene (analyte **4**), the excitation wavelength of 265 nm is a wavelength at which compounds **1**, **8**, and **9** have noticeable absorption cross-sections (see ESI†). Although significant wavelength-dependent fluorescence decreases were observed, these observed changes are indicative of an inner filter mechanism, where the macrocycle absorbs energy and filters some of that energy from reaching the analyte.[35]

The limits of detection of analytes **4–7** using this method were calculated following literature-reported procedures (Table 2).[36] For analyte **4**, the calculated detection limit is a result of the inner filter effect-induced fluorescence changes.[35] The nanomolar detection limits obtained for the analytes are close to or below the literature-reported levels of concern for three out of the four analytes (compounds **4**, **5**, and **7**),[37] which highlights

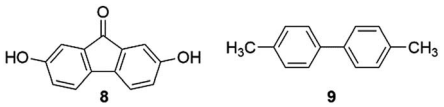

Fig. 4 Structures of photophysically active components **8** and **9** (structurally tethered in **1**).

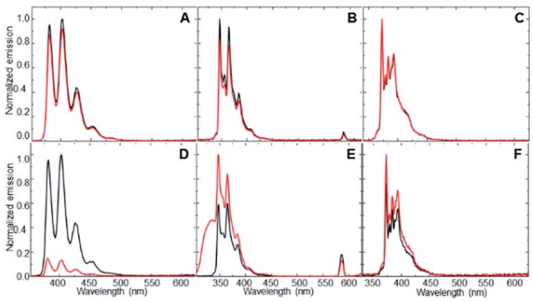

Fig. 5 Fluorescence emission changes of analytes **5**–**7** in the presence of macrocycle **1** (A–C) and component moieties **8** and **9** (D–F). (A and D) Analyte **5**; (B and E) analyte **6**; and (C and F) analyte **7**. The black line represents the fluorescence emission from the analyte alone, and the red line represents the fluorescence emission from the analyte in the presence of the other compounds.

the high sensitivity of this fluorescence method for PAH binding and concomitant detection. The limits of detection for the analytes in the absence of the macrocycle were higher, which highlights the role of the macrocycle in enhancing fluorescence sensitivities.

In addition to binding PAHs in the cavity interior, macrocycle **1** (10 μM in DMSO) was also investigated for its ability to bind anions. Among all anions studied (fluoride, cyanide, azide, and thiocyanate), only fluoride exhibited a noticeable spectroscopic change (Fig. 6) with increases in the molar absorptivity of the macrocycle's λ_{max} bands at 264 and 305 nm. The response for fluoride is likely due to its ability to act as a hydrogen bond acceptor, as a result of its small size, high electronegativity, and high charge density.[40]

The fluoride binding was confirmed by nonlinear curve fitting of the NMR titration data to host-guest binding models (Fig. 7 and Table 3). An excellent non-linear fit was obtained for a 1 : 2 binding stoichiometry between macrocycle **1** and two fluoride anions, and this stoichiometry was confirmed with a Job plot analysis that showed a maximum at a molar ratio of 0.66 (see ESI† for details). The calculated binding constants

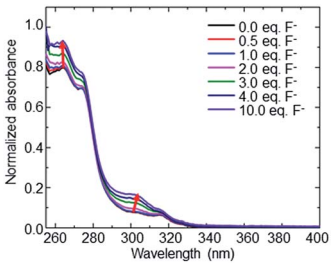

Fig. 6 Illustration of changes in the UV-visible absorption spectrum of macrocycle **1** with the addition of up to 10 equivalents of fluoride anion.

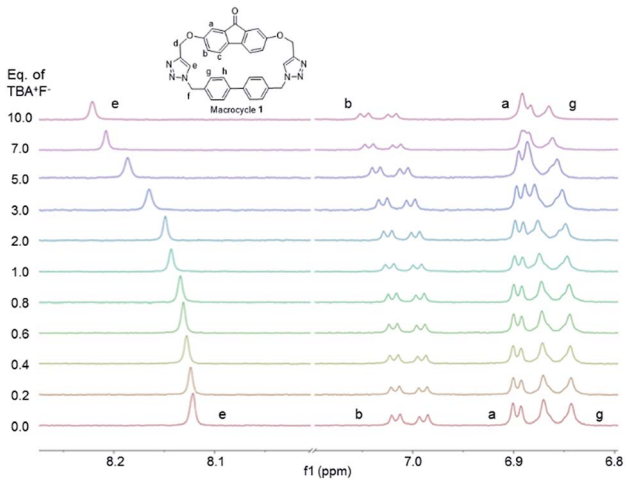

Fig. 7 Illustration of changes in the ^{1}H NMR chemical shifts of macrocycle **1** with the titration of fluoride anions.

indicate anti-cooperativity, with the binding of the first fluoride (K_1 = 522 M^{-1}) preferred compared to binding of the second fluoride anion (K_2 = 333.25 M^{-1}). This phenomenon could be attributed to the fact that the fluorenone flexibility is constrained by the first binding, reducing the conformational flexibility for the second fluoride binding. Each fluoride anion interacts with the triazole proton (H_e, red), and is additionally assisted by the fluorenone and biphenyl protons (H_b, blue and H_g, green) (Fig. 8), as shown through the chemical shift changes of these protons with the addition of up to 10 equivalents of fluoride anion (Table 3).

The small size of fluoride makes it compatible with the binding pockets in each arm of the macrocycle. This

Table 2 Limits of detection for analytes **4**–**7** and comparisons to literature-reported values

Analyte	Limit of detection with compound **1**[a] (nM)	Limit of detection without compound **1**[a] (nM)	Literature-reported values (nM)
4	28.7 ± 0.1	166.5 ± 1.4	78.0 (ref. 38)
5	2.2 ± 0.8	30.1 ± 0.9	0.8 (ref. 39)
6	37.2 ± 0.1	59.5 ± 0.7	0.6 (ref. 38)
7	4.2 ± 0.0	204.8 ± 1.1	0.8 (ref. 39)

[a] Details for the limit of detection calculations can be found in the ESI. All results represent an average of at least 3 trials.

Table 3 Illustration of the changes in the ^{1}H NMR chemical signal of macrocycle **1** with binding of fluoride anions[a]

	Change in δ (ppm)			
Equivalents of fluoride	H_e	H_b	H_a	H_g
1	0.014	0.004	−0.000	0.002
3	0.044	0.016	−0.003	0.009
5	0.066	0.022	−0.005	0.014
10	0.100	0.031	−0.010	0.022

[a] Detailed methods for the ^{1}H NMR titration are shown in the ESI.

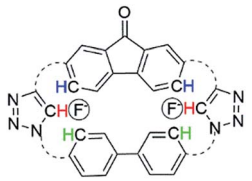

Fig. 8 Proposed geometry of how macrocycle **1** binds two fluoride anions.

Table 4 Illustration of the changes in the ^{1}H NMR chemical signal of triazole proton with the binding of 10 equivalents of anions[a]

Anion	$\Delta\delta$ (ppm)
F^-	0.1002
CN^-	0.0021
SCN^-	0.0025
N_3^-	0.0024

[a] Detailed methods for the ^{1}H NMR titration are shown in the ESI.

compatibility results in selective binding of fluoride, with significantly higher chemical shift changes compared to the other anions (Table 4).

Moreover, the solvent used in these NMR titration experiments has a significant effect on the magnitude of the shifts observed. Chemical shift changes of higher magnitude have been reported in the literature with $[HF_2]^-$ and triazolophane hosts in deuterated dichloromethane.[41] Because of solubility constraints, binding analyses were carried out in d_6-DMSO. Even though hydrogen fluoride and HF_2^- anions are present to a minor extent, their relatively small amounts (see ESI†) means that they are unlikely to have a significant effect on fluoride binding. Moreover, chemical shift changes of the tetrabutylammonium indicated no significant association between the counterion and the macrocycle–fluoride complex.

In conclusion, we have successfully synthesized a new macrocycle composed of biphenyl and fluorenone moieties linked by two triazoles. We demonstrated that macrocycle **1** is sensitive towards small amounts of PAHs with limits of detections in the nanomolar range. Additionally, compound **1** is able to bind selectively to fluoride in 2 : 1 stoichiometry through the use of triazole, fluorenone and biphenyl-facilitated C–H binding. This macrocycle can be used as a scaffold for additional detection applications as well as a crucial tool in our efforts to understand fundamental intermolecular interactions. Results of these and other investigations are currently underway in our laboratory, and results will be reported in due course.

Acknowledgements

The authors acknowledge Dr Li Li (MIT) and the Smith-Oxley research group (University of Rhode Island) for their help with mass spectrometry. This research was supported by the University of Rhode Island Department of Chemistry.

Notes and references

1 E. J. Dale, N. A. Vermeulen, M. Juricek, J. C. Barnes, R. M. Young, M. R. Wasielewski and J. F. Stoddart, *Acc. Chem. Res.*, 2016, **49**, 262.
2 J. C. Barnes, M. Juricek, N. L. Strutt, M. Frasconi, S. Sampath, M. A. Giesener, P. L. McGrier, C. J. Bruns, C. L. Stern, A. A. Sarjeant and J. F. Stoddart, *J. Am. Chem. Soc.*, 2013, **135**, 183.
3 A. Kim, R. Ali, S. H. Park, Y.-H. Kim and J. S. Park, *Chem. Commun.*, 2016, **52**, 11139.
4 E. Makrlik, S. Bohm, D. Sykora, B. Klepetarova, V. Petr and M. Polasek, *Chem. Phys. Lett.*, 2015, **642**, 39.
5 D. J. Cram, C. S. Montgomery and G. R. Knox, *J. Am. Chem. Soc.*, 1966, **88**, 515.
6 S.-i. Kato, N. Yamazaki, T. Tajima and Y. Nakamura, *Chem. Lett.*, 2013, **42**, 401.
7 M. Busch, M. Cayir, M. Nieger, W. R. Thiel and S. Brase, *Eur. J. Org. Chem.*, 2013, **2013**, 6108.
8 F. Wei, W. Wang, Y. Ma, C.-H. Tung and Z. Xu, *Chem. Commun.*, 2016, **52**, 14188.
9 Y. H. Lau, P. J. Rutledge, M. Watkinson and M. H. Todd, *Chem. Soc. Rev.*, 2011, **40**, 2848.
10 J. Cai and J. L. Sessler, *Chem. Soc. Rev.*, 2014, **43**, 6198.
11 L. S. Thakur and P. Semil, *Int. J. ChemTech Res.*, 2013, **5**, 1299.
12 C. A. Palmer and J. A. Gilbert, *J. Acad. Nutr. Diet.*, 2012, **112**, 1443.
13 M. Borysewicz-Lewicka and J. Opydo-Szymaczek, *Pol. J. Environ. Stud.*, 2016, **25**, 9.
14 H. Komaba and M. Fukagawa, *Kidney Int.*, 2016, **90**, 753.
15 A. H. Gorenjak and A. Cencic, *Acta Aliment.*, 2013, **42**, 158.
16 T. J. Barrett and C. L. Hawkins, *Chem. Res. Toxicol.*, 2012, **25**, 263.
17 R. Jackson and B. A. Logue, *Anal. Chim. Acta*, 2017, **960**, 18.
18 D. M. Badgujar, M. B. Talawar, S. N. Asthana and P. P. Mahulikar, *J. Hazard. Mater.*, 2008, **151**, 289.
19 S. Marzooghi and D. M. Di Toro, *Environ. Toxicol. Chem.*, 2017, **36**, 1138–1148.
20 L. D. Claxton, *Mutat. Res., Rev. Mutat. Res.*, 2014, **762**, 108.
21 A. J. Mearns, D. J. Reish, P. S. Oshida, T. Ginn, M. A. Rempel-Hester, C. Arthur, N. Rutherford and R. Pryor, *Water Environ. Res.*, 2015, **87**, 1718.
22 N. Verma, M. Pink, A. W. Rettenmeier and S. Schmitz-Spanke, *Proteomics*, 2012, **12**, 1731.

23 E. B. Balcioglu, *Toxin Rev.*, 2016, **35**, 98.
24 C. Ceccaroli, A. Pulliero, M. Geretto and A. Izzotti, *J. Environ. Sci. Health, Part C: Environ. Carcinog. Ecotoxicol. Rev.*, 2015, **33**, 188.
25 N. Serio, D. F. Moyano, V. M. Rotello and M. Levine, *Chem. Commun.*, 2015, **51**, 11615.
26 D. J. DiScenza and M. Levine, *Supramol. Chem.*, 2016, **28**, 881; D. J. DiScenza and M. Levine, *New J. Chem.*, 2016, **40**, 789.
27 B. Radaram and M. Levine, *Eur. J. Org. Chem.*, 2015, **2015**, 6194; B. Radaram, J. Potvin and M. Levine, *Chem. Commun.*, 2013, **49**, 8259.
28 P. Knops, N. Sendhoff, H. B. Mekelburger and F. Voegtle, *Top. Curr. Chem.*, 1992, **161**, 1.
29 T. Ohana, M. Kaise, S. Nimura, O. Kikuchi and A. Yabe, *Chem. Lett.*, 1993, 765.
30 W.-L. Yu, J. Pei, W. Huang and A. J. Heeger, *Adv. Mater.*, 2000, **12**, 828.
31 F. Uckert, S. Setayesh and K. Mullen, *Macromolecules*, 1999, **32**, 4519.
32 J. Y. Kwon, N. J. Singh, H. N. Kim, S. K. Kim, K. S. Kim and J. Yoon, *J. Am. Chem. Soc.*, 2004, **126**, 8892.
33 H.-D. Becker, C. Burgdorff and H.-G. Loehmannsroeben, *J. Photochem. Photobiol., A*, 1995, **86**, 133.
34 Y.-H. Chen, K.-C. Tang, Y.-T. Chen, J.-Y. Shen, Y.-S. Wu, S.-H. Liu, C.-S. Lee, C.-H. Chen, T.-Y. Lai, S.-H. Tung, R.-J. Jeng, W.-Y. Hung, M. Jiao, C.-C. Wu and P.-T. Chou, *Chem. Sci.*, 2016, **7**, 3556.
35 F. Akhgari, N. Samadi and K. Farhadi, *J. Fluoresc.*, 2017, **27**, 921–927; P. Marks, B. Radaram, M. Levine and I. A. Levitsky, *Chem. Commun.*, 2015, **51**, 7061.
36 B. Saute and R. Narayanan, *J. Raman Spectrosc.*, 2013, **44**, 1518.
37 K. Blasch, J. Kolivosky and B. Hill, *Inhalation Toxicol.*, 2016, **28**, 216.
38 Center for Disease Control and Prevention, *The National Institute for Occupational Safety and Health (NIOSH): Naphthalene*, https://www.cdc.gov/niosh/npg/npgd0439.html, accessed, Mar 27, 2017.
39 Center for Disease Control and Prevention, *The National Institute for Occupational Safety and Health (NIOSH): Coal tar pitch volatiles*, https://www.cdc.gov/niosh/npg/npgd0145.html, accessed, Mar 27, 2017.
40 M. Cametti and K. Rissanen, *Chem. Commun.*, 2009, 2809.
41 R. O. Ramabhadran, Y. Liu, Y. Hua, M. Ciardi, A. H. Flood and K. Raghavachari, *J. Am. Chem. Soc.*, 2014, **136**, 5078.